Journal of Modern Optics

ISSN: 0950-0340 (Print) 1362-3044 (Online) Journal homepage: http://www.tandfonline.com/loi/tmop20

Producing optical vortices through forked holographic grating: study of polarization

Virendra K. Jaiswal , Ravindra P. Singh & R. Simon

To cite this article: Virendra K. Jaiswal , Ravindra P. Singh & R. Simon (2010) Producing optical vortices through forked holographic grating: study of polarization, Journal of Modern Optics, 57:20, 2031-2038, DOI: 10.1080/09500340.2010.515748

To link to this article: http://dx.doi.org/10.1080/09500340.2010.515748

Journal of Modern Optics
Vol. 57, No. 20, 20 November 2010, 2031–2038

Taylor & Francis
Taylor & Francis Group

Producing optical vortices through forked holographic grating: study of polarization

Virendra K. Jaiswal[a]*, Ravindra P. Singh[b] and R. Simon[c]

[a]*Optical Radiation Standards, National Physical Laboratory, New Delhi – 110012, India;* [b]*Theoretical Physics Division, Physical Research Laboratory, Ahmedabad – 380009, India;* [c]*The Institute of Mathematical Sciences, C.I.T. Campus, Taramani, Chennai – 600113, India*

(*Received 13 February 2010; final version received 5 August 2010*)

It is important to know what happens to initial polarization during the formation of optical vortices. We use a computer-generated forked holographic grating to produce optical vortices in the laboratory and study changes in polarization, introduced by the grating, which generates optical vortices in its diffracted orders. The Mueller matrix has been used to quantify changes in the polarization in diffracted orders containing optical vortices. Decomposition of the Mueller matrices estimates the polarizing properties, such as diattenuation, retardance and depolarization of the system. We find that the system is a non-depolarizing system. The study also shows that spin and the orbital angular momentum of photons are not coupled in this process.

Keywords: optical vortices; polarization; diffraction gratings

1. Introduction

In general, light beams emitted by most lasers are described by Hermite–Gaussian beams; however, several other beams have been found as a solution to Maxwell's equations for electromagnetic waves. One of the very important beams is an optical vortex, a manifestation of phase singularity in the optical field [1]. It should be noted that phase singularities are found throughout optical physics. They arise naturally in diffraction patterns, speckle fields and various other natural phenomena when light passes through a rough surface, or due to phase modification when light propagates through a medium. However, to produce the phase singularities in a controlled manner one requires devices such as computer-generated holograms [2] (CGHs), spiral phase plates [3] and mode converters [4].

An optical vortex is a kind of singularity that runs parallel to the beam axis. The phase around the vortex is given by $\exp(il\phi)$, where l can be any integer value, known as topological charge of the vortex. The associated phase fronts are inclined with respect to the beam axis, resulting in the azimuthal component of the momentum flow, thus giving orbital angular momentum to photons in the light beam. Because of their specific spatial structure, associated helical wave front and orbital angular momentum [5], they find a variety of applications in the optical trapping of atoms [6], optical tweezers [7,8], optical spanners [9], micro-machining [10] and optical communication [11]. Recently, they have also found applications in quantum computation and quantum information [12,13]. Despite having so many applications, their physical properties are still not very well understood, polarization being an example. Optical vortices are regarded as phase defects in a scalar electromagnetic wave field [14]. For a vector field that takes into account polarization of the wave, polarization singularities have been studied [14,15]. However, one is not clear what happens to the polarization of the incident light that is transformed into an optical vortex after diffraction from a phase object, most often a forked holographic grating. We have carried out this investigation with optical vortices produced from a computer-generated hologram (CGH) by changing the polarization of the incident TEM_{00} mode of a HeNe laser beam. To our knowledge, this is the first time it has been shown that the forked holographic grating changes the polarization in the process of forming the vortex. The changes in polarization have been analyzed with the help of Mueller matrices.

2. Experiment

The experimental setup for investigating the polarization properties of optical vortices is shown in Figure 1. The TEM_{00} mode of an intensity stabilized 1 mW red HeNe laser (Melles Griot, 117A) was passed through the polarizer, P1, whose pass axis is set to be vertical, and a quarter-wave plate, QWP1, to select the incident

*Corresponding author. Email: jaiswalvk@mail.nplindia.ernet.in

ISSN 0950–0340 print/ISSN 1362–3044 online

DOI: 10.1080/09500340.2010.515748
http://www.informaworld.com

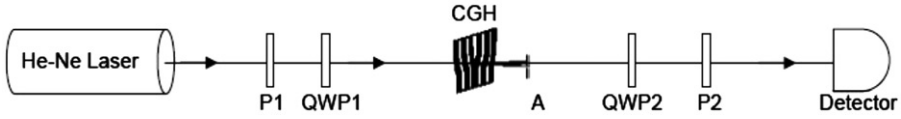

Figure 1. Schematic diagram of experimental arrangement. P1, P2, polarizers; QWP1, QWP2, quarter-wave plates; CGH, computer-generated hologram and A, aperture.

polarization used to generate the optical vortex. After preparing the incident light in a particular state of polarization by changing the angle between P1 and QWP1, it was passed through the branch point of the computer-generated forked grating hologram. The holographic sheets were procured from Geola (PFG-03M). The diffraction produced consists of optical vortices in different orders as well as a Hermite–Gaussian (HG_{00}) in central order. The first orders of diffraction on either side of the center correspond to vortices of order one, but with opposite topological charge. The sign and order of the vortices were confirmed by observing the interference of the vortex with a plane wave in a Mach–Zehnder interferometer [16]. Diffraction orders were selected one by one through an aperture A to study the nature of their polarization.

To study the polarization of the beams obtained by diffraction from the CGH, a polarizer, P2, and quarter-wave plate, QWP2, were used. Various components of polarization – horizontal, vertical, +45°, −45°, right-handed (RH) and left-handed (LH) circular polarization were measured as prescribed for finding the Stokes vector [17]. Horizontal, vertical, +45°, and −45° components were measured with the polarizer, P2, in horizontal, vertical, +45°, and −45° orientations with respect to the pass axis of polarizer, P1, while the right-handed (RH) and left-handed (LH) circular components of polarization were measured with the insertion of a quarter-wave plate, QWP2, between the aperture A and polarizer P2 keeping P2 in +45° and −45° orientations. The fast axis of QWP2 was fixed parallel to the pass axis of P1. The process of taking observations is repeated for each order, changing polarization of the incident beam – horizontal linear, vertical linear, +45° linear, −45° linear, left circular, right circular, and ±15°, ±30°, ±60°, ±75° elliptical. Observations for each orientation are recorded in terms of intensity measured in microwatts by an ILX Lightwave OMM 6810-B optical multimeter with silicon power head, OMH-6701-B. Each component of polarization is divided by the corresponding total linear (or circular) polarized light present in the diffraction order and the fraction is plotted with the changing polarization of the incident beam as shown in Figures 2–4. These observations were repeated to reduce the uncertainty of measurements and are shown with vertical error bars in the plots.

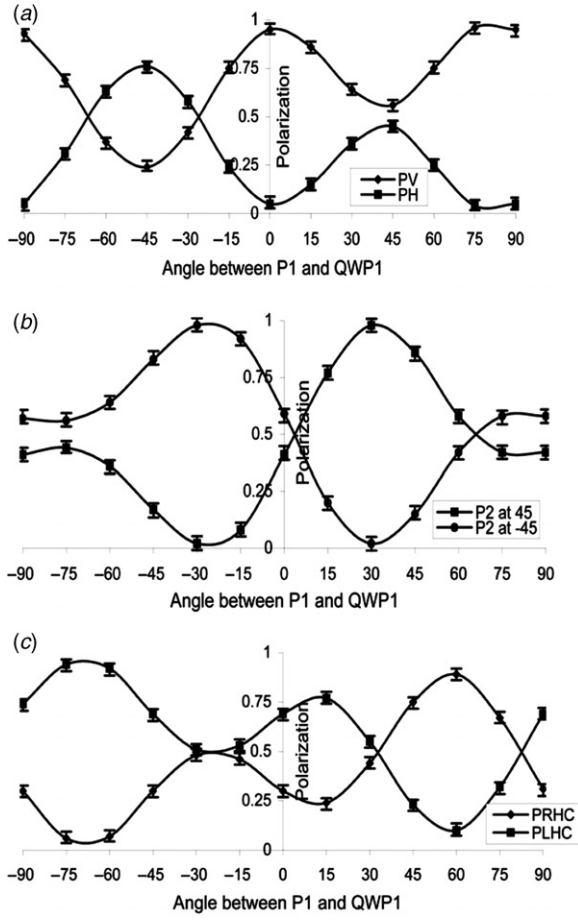

Figure 2. Variation of different polarization components in −1 order with changes in incident polarization (*a*) PH: horizontal, PV: vertical, (*b*) P2 at 45°, P2 at −45° with pass axis of P1, and (*c*) PLHC: left-hand circular, PRHC: right-hand circular.

3. Results and discussion

Let us first analyze the nature of polarization observed for the vortex of topological charge −1. Figure 2(*a*)

shows the plot for components of polarization, which are parallel (vertical) and perpendicular (horizontal) to the pass axis of polarizer P1. One can see that both the components follow different paths and their values depend on incident polarization. The plots in Figure 2(*b*) show the behavior of polarization components, which are at $+45^\circ$ and -45° to the pass axis of P1. It is interesting to note the crossing of two polarization components in Figure 2(*a*) as well as Figure 2(*b*). Therefore, at these points, one cannot say if the polarization of the diffracted order is vertical or horizontal; $+45^\circ$ linear or -45° linear. It reminds us of the nature of polarization of down-converted photons [18,19] where a photon has an equal probability of being vertically or horizontally polarized. Right-handed circular polarization (RHC) and left-handed circular polarization (LHC) components measured using P2 and QWP2 are shown in Figure 2(*c*). These components not only cross each other twice for positive helicity of incident polarization but also approach a common value when the helicity was reversed, again giving three possible points where a detected photon could have equal probability of being left circularly polarized or right circularly polarized. We also find, as observed in earlier experiments [20–22] the presence of a cross-polarization component in central order, which is the lowest-order Hermite–Gaussian beam.

The same polarization behavior for the central order and vortex signifies that polarization, which is the spin angular momentum of a photon, is not coupled with the orbital angular momentum of a photon [23], which is characteristic of photons in an optical vortex. The behaviors of various polarization components with changing incident polarization for vortices of orders -1, $+1$ and central order are shown in Figures 2–4.

The measured polarization components were used to calculate sets of input and output Stokes vectors for each order. These Stokes vectors were used to obtain Mueller matrices with the method of least squares. The Mueller matrix M_{-1} for the vortex of order -1 turns out to be,

$$\mathrm{M}_{-1} = \begin{pmatrix} 0.0456 & 0.0018 & -0.0001 & -0.0018 \\ 0.0000 & 0.0397 & -0.0046 & 0.0183 \\ -0.0003 & -0.0063 & 0.0373 & 0.0315 \\ -0.0011 & -0.0161 & -0.0325 & 0.0214 \end{pmatrix}. \tag{1}$$

Using the known algorithm [24,25], the Mueller matrix in Equation (1) was further decomposed into diattenuation ($\mathrm{M}_{-1\mathrm{D}}$), retardance ($\mathrm{M}_{-1\mathrm{R}}$), and depolarization ($\mathrm{M}_{-1\Delta}$) matrices. In fact, diattenuation of an optical element characterizes the dependence of intensity transmittance on the polarization state of the incident beam. The intensity transmittance is a maximum for one eigenpolarization state, and a minimum for the other (orthogonal) eigenpolarization state. The direction of eigenpolarization along which intensity transmission is maximum, is defined as the axis of diattenuation. A diattenuator has a symmetric Mueller matrix defined by

$$\mathrm{M_D} = \begin{bmatrix} 1 & \vec{\mathrm{D}}^{\mathrm{T}} \\ \vec{\mathrm{D}} & \mathrm{m_D} \end{bmatrix},$$

$\mathrm{m_D} = \sqrt{1-\mathrm{D}^2}\,\mathrm{I} + (1-\sqrt{1-\mathrm{D}^2})\hat{\mathrm{D}}\hat{\mathrm{D}}^{\mathrm{T}}$, where I is a 3×3 identity matrix, T denotes the transposition, $\vec{\mathrm{D}}$ is a diattenuation vector and $\hat{\mathrm{D}}$ is its unit vector and they are defined as

$$\vec{\mathrm{D}} = \frac{1}{m_{00}}[m_{01}\ m_{02}\ m_{03}]^{\mathrm{T}}, \quad \hat{\mathrm{D}} = \frac{\vec{\mathrm{D}}}{\left|\vec{\mathrm{D}}\right|},$$

m_{ij} is a matrix element of the ith row and jth column of the initial Mueller matrix M normalized with the element m_{00}.

A retarder introduces different phase changes for its orthogonal polarizations and the difference in phase changes is a measure of its retardance. The direction of retardance (or fast axis) of the retarder is along the eigenpolarization that emerges first from the retarder. A retarder has a Mueller matrix given by

$$\mathrm{M_R} = \begin{pmatrix} 1 & \vec{0}^{\mathrm{T}} \\ \vec{0} & \mathrm{m_R} \end{pmatrix},$$

where $\mathrm{m_R}$ is a 3×3 sub matrix of $\mathrm{M_R}$, $\vec{0}$ is a 3×1 column matrix and T denotes transposition. The retardance is given by

$$\mathrm{R} = \cos^{-1}\left[\frac{\mathrm{Tr(M_R)}}{2} - 1\right]$$

where $\mathrm{Tr(M_R)}$ denotes trace of matrix $\mathrm{M_R}$.

The depolarizing property of a polarizing element can be characterized with the power of depolarization of the element. The most general form for a Mueller matrix of a pure depolarizer is given by

$$\mathrm{M}_\Delta = \begin{pmatrix} 1 & \vec{0}^{\mathrm{T}} \\ \vec{\mathrm{P}}_\Delta & \mathrm{m}_\Delta \end{pmatrix}$$

where $\vec{\mathrm{P}}_\Delta$ denotes the polarizance vector, which characterizes the polarizing capability of the depolarizer. The eigenvectors of the sub matrix m_Δ give the three principal axes of the depolarizer. The depolarization

power is given by

$$\Delta = 1 - \frac{|\mathrm{Tr}(\mathrm{M}_\Delta) - 1|}{3}$$

where $\mathrm{Tr}(\mathrm{M}_\Delta)$ denotes the trace of matrix M_Δ. For a vortex of order −1, these matrices can be written as

$$\mathrm{M}_{-1\mathrm{D}} = \begin{pmatrix} 1 & 0.0395 & -0.0022 & -0.0395 \\ 0.0395 & 0.9992 & -0.0000 & -0.0008 \\ -0.0022 & -0.0000 & 0.9984 & 0.0000 \\ -0.0395 & -0.0008 & 0.0000 & 0.9992 \end{pmatrix},$$

$$\mathrm{M}_{-1\mathrm{R}} = \begin{pmatrix} 1 & 0 & 0 & 0 \\ 0 & 0.9021 & -0.1470 & 0.4056 \\ 0 & -0.1960 & 0.6978 & 0.6890 \\ 0 & -0.3843 & -0.7010 & 0.6007 \end{pmatrix},$$

$$\mathrm{M}_{-1\Delta} = \begin{pmatrix} 1 & 0 & 0 & 0 \\ -0.0188 & 0.9648 & 0.0351 & -0.0232 \\ 0.0281 & 0.0351 & 1.0759 & -0.1052 \\ 0.0068 & -0.0232 & -0.1052 & 0.9183 \end{pmatrix}.$$

Figures 3 and 4 show the nature of various polarization components for the central order and the vortex of topological charge +1. They follow the same pattern as observed for the vortex of topological charge −1 shown in Figure 2 and discussed above. The Mueller matrix and its decomposition for these orders are

$$\mathrm{M}_0 = \begin{pmatrix} 0.0770 & 0.0003 & 0.0001 & 0.0003 \\ 0.0001 & 0.0684 & -0.0080 & 0.0314 \\ 0.0003 & -0.0119 & 0.0644 & 0.0537 \\ 0.0001 & -0.0282 & -0.0547 & 0.0351 \end{pmatrix}$$

$$\mathrm{M}_{0\mathrm{D}} = \begin{pmatrix} 1 & 0.0039 & 0.0013 & 0.0039 \\ 0.0039 & 1.0000 & 0.0000 & 0.0000 \\ 0.0013 & 0.0000 & 1.0000 & 0.0000 \\ 0.0039 & 0.0000 & 0.0000 & 1.0000 \end{pmatrix},$$

$$\mathrm{M}_{0\mathrm{R}} = \begin{pmatrix} 1 & 0 & 0 & 0 \\ 0 & 0.8970 & -0.1488 & 0.4163 \\ 0 & -0.2027 & 0.6984 & 0.6864 \\ 0 & -0.3928 & -0.7001 & 0.5963 \end{pmatrix},$$

$$\mathrm{M}_{0\Delta} = \begin{pmatrix} 1 & 0 & 0 & 0 \\ -0.0036 & 0.9820 & 0.0273 & -0.0331 \\ 0.0007 & 0.0273 & 1.0942 & -0.1090 \\ 0.0019 & -0.0331 & -0.1090 & 0.9130 \end{pmatrix}$$

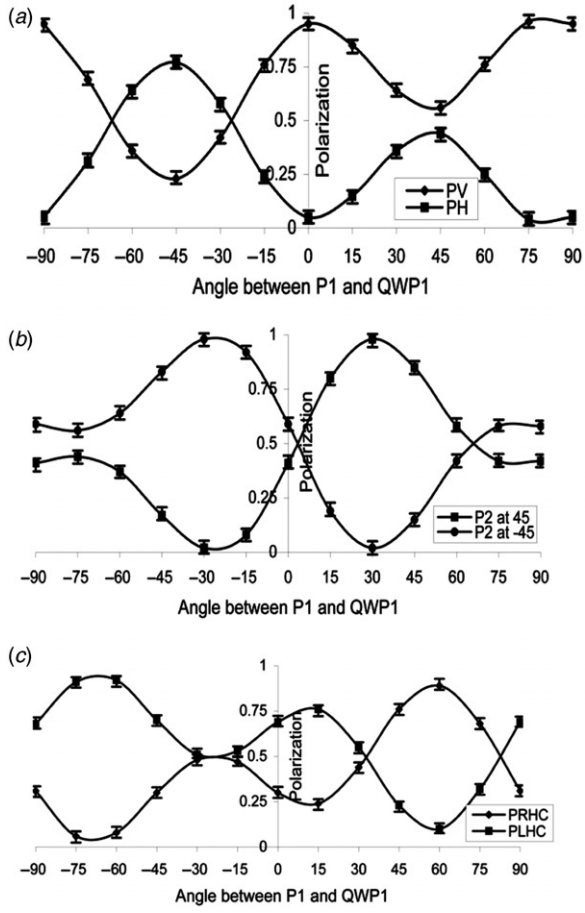

Figure 3. Variation of different polarization components in central order with changes in incident polarization (*a*) PH: horizontal, PV: vertical; (*b*) P2 at 45°, P2 at −45° with pass axis of P1; and (*c*) PLHC: left-hand circular, PRHC: right-hand circular.

and

$$\mathrm{M}_{+1} = \begin{pmatrix} 0.0480 & 0.0039 & -0.0006 & 0 \\ 0.0011 & 0.0425 & -0.0046 & 0.0197 \\ -0.0004 & -0.0070 & 0.0398 & 0.0335 \\ -0.0004 & -0.0178 & -0.0341 & 0.0215 \end{pmatrix}$$

$$\mathrm{M}_{+1\mathrm{D}} = \begin{pmatrix} 1.0000 & 0.0812 & -0.0125 & 0 \\ 0.0812 & 1.0000 & -0.0005 & 0 \\ -0.0125 & -0.0005 & 0.9967 & 0 \\ 0 & 0 & 0 & 0.9966 \end{pmatrix},$$

$$\mathrm{M}_{+1\mathrm{R}} = \begin{pmatrix} 1 & 0 & 0 & 0 \\ 0 & 0.8962 & -0.1506 & 0.4172 \\ 0 & -0.2036 & 0.6960 & 0.6886 \\ 0 & -0.3941 & -0.7020 & 0.5931 \end{pmatrix},$$

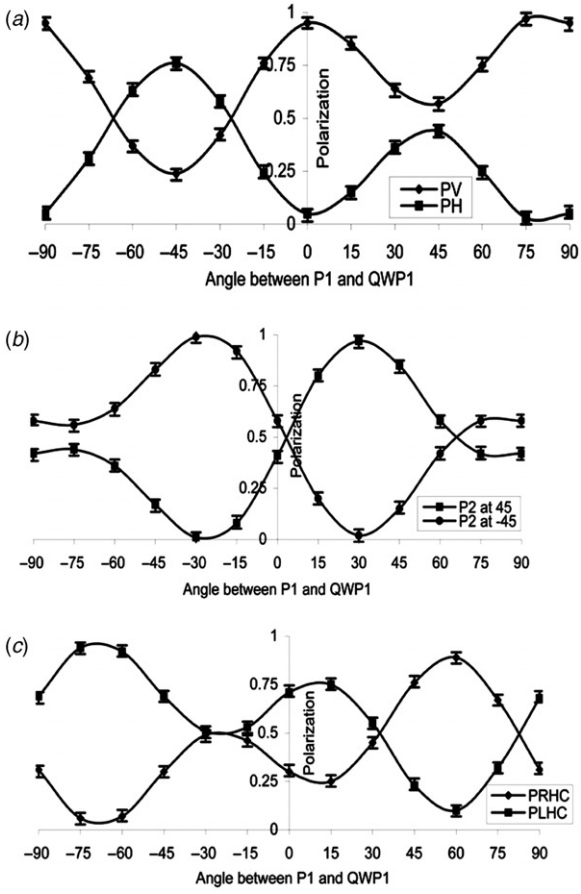

Figure 4. Variation of different polarization components in +1 order with changes in incident polarization (*a*) PH: horizontal, PV: vertical; (*b*) P2 at 45°, P2 at −45° with pass axis of P1; and (*c*) PLHC: left-hand circular, PRHC: right-hand circular.

$$M_{+1\Delta} = \begin{pmatrix} 1 & 0 & 0 & 0 \\ -0.0505 & 0.9835 & 0.0355 & -0.0387 \\ 0.0140 & 0.0355 & 1.0911 & -0.1109 \\ 0.0130 & -0.0387 & -0.1109 & 0.9137 \end{pmatrix}.$$

We obtain diattenuation to be 0.082, retardance as 0.934 radian and depolarization to be 0.004 for the vortex of order +1. For the central order and vortex of order −1 these values are 0.006, 0.932 radian, 0.004 and 0.056, 0.927 radian, 0.014, respectively.

However, the decomposition of the Mueller matrix does not make any sense if our experimentally obtained Mueller matrices are not bona fide Mueller matrices. To see if our experimental Mueller matrices qualify to be the Mueller matrix of a linear system we check that each of our Mueller matrix maps an input pure state Stokes vector with unit intensity into a Stokes vector with degree of polarization p that satisfies the condition [26], $0 \le p \le 1$. We do confirm that for each of our Mueller matrix M_{-1}, M_0, and M_{+1}, $m_{00} \ge \sqrt{(m_{01}^2 + m_{02}^2 + m_{03}^2)}$. The plots for $p(\theta, \varphi)$ in Figure 5(*a*)–(*c*) shows $p \le 1$ in general, except for small regions where p is slightly greater than 1 within experimental errors. This confirms that our Mueller matrices are bona fide Mueller matrices representing a physical system.

Now, we calculate the N matrices [27–29] for corresponding Mueller matrices M_{+1}, M_0, and M_{-1}:

$$N_{+1} = \begin{bmatrix} 0.0477 & -0.0026 + 0.0098i & -0.0037 + 0.0091i & 0.0306 + 0.0338i \\ -0.0026 - 0.0098i & 0.0013 & 0.0091 + 0.0003i & 0.0033 - 0.0087i \\ -0.0037 - 0.0091i & 0.0091 - 0.0003i & 0.0041 & 0.0020 - 0.0098i \\ 0.0306 - 0.0338i & 0.0033 + 0.0087i & 0.0020 + 0.0098i & 0.0427 \end{bmatrix},$$

$$N_0 = \begin{bmatrix} 0.0729 & -0.0039 + 0.0158i & -0.0058 + 0.0140i & 0.0497 + 0.0542i \\ -0.0039 - 0.0158i & 0.0042 & 0.0146 + 0.0005i & 0.0061 - 0.0141i \\ -0.0058 - 0.0140i & 0.0146 - 0.0005i & 0.0044 & 0.0040 - 0.0155i \\ 0.0497 - 0.0542i & 0.0061 + 0.0141i & 0.0040 + 0.0155i & 0.0725 \end{bmatrix},$$

$$N_{-1} = \begin{bmatrix} 0.0435 & -0.0023 + 0.0082i & -0.0033 + 0.0086i & 0.0293 + 0.0320i \\ -0.0023 - 0.0082i & 0.0020 & 0.0079 + 0.0005i & 0.0030 - 0.0075i \\ -0.0033 - 0.0086i & 0.0079 - 0.0005i & 0.0038 & 0.0022 - 0.0100i \\ 0.0293 - 0.0320i & 0.0030 + 0.0075i & 0.0022 + 0.0100i & 0.0417 \end{bmatrix}.$$

and verify the condition $\mathrm{Tr(N).N} = \mathrm{N}^2$ for the first order,

$$\mathrm{Tr}(\mathrm{N}_{+1}) \cdot \mathrm{N}_{+1} = \begin{bmatrix} 0.0046 & -0.0002 + 0.0009\mathrm{i} & -0.0004 + 0.0009\mathrm{i} & 0.0029 + 0.0032\mathrm{i} \\ -0.0002 - 0.0009\mathrm{i} & 0.0001 & 0.0009 + 0.000\mathrm{i} & 0.0003 - 0.0008\mathrm{i} \\ -0.0004 - 0.0009\mathrm{i} & 0.0009 - 0.000\mathrm{i} & 0.0004 & 0.0002 - 0.0009\mathrm{i} \\ 0.0029 - 0.0032\mathrm{i} & 0.0003 + 0.0008\mathrm{i} & 0.0002 + 0.0009\mathrm{i} & 0.0041 \end{bmatrix}$$

$$\cong \mathrm{N}_{+1}^2 = \begin{bmatrix} 0.0046 & -0.0004 + 0.0009\mathrm{i} & -0.0005 + 0.0009\mathrm{i} & 0.0029 + 0.0032\mathrm{i} \\ -0.0004 - 0.0009\mathrm{i} & 0.0003 & 0.0002 + 0.0000\mathrm{i} & 0.0004 - 0.0009\mathrm{i} \\ -0.0005 - 0.0009\mathrm{i} & 0.0002 - 0.0000\mathrm{i} & 0.0003 + 0.0000\mathrm{i} & 0.0003 - 0.0009\mathrm{i} \\ 0.0029 - 0.0032\mathrm{i} & 0.0004 + 0.0009\mathrm{i} & 0.0003 + 0.0009\mathrm{i} & 0.0041 + 0.0000\mathrm{i} \end{bmatrix}.$$

We find that the condition is satisfied within experimental uncertainties. Similarly, other orders also satisfy the above criterion, implying that the system is a non-depolarizing system.

In calculating the Mueller matrix elements it is very much desirable to point out the possible sources of errors and experimental uncertainties. A considerable amount of work has been devoted to the calculation of errors in determining the Mueller matrix elements [30,31]. One of the most important sources of error is misalignment of retarders. A 5 minute misalignment can lead to 2% of error in the Mueller matrix elements. The detection accuracy of the detector, source power fluctuations, the optical elements not being normal to the beam, multiple reflections and backlash error in the optical mounts are other possible sources of errors. In addition, non-planer surfaces of the optical elements on rotation may lead to beam wandering, which could be another source of error. In our experiment, the least count of the rotating optical mounts is 5 minutes. The fluctuation in the laser intensity is $\pm 0.05\%$, and the power measurement accuracy of the Silicon power head is $\pm 3\%$.

Figure 6 shows the variation in degree of polarization for linear and circular components of polarization for each order: (*a*) vortex of charge -1; (*b*) central order; and (*c*) vortex of order $+1$ with incident polarization. One can see that variations in the degree of polarization for circular as well as linear polarized light follow the same trend for all three orders while the polarization of incident light is changed. However, the variation of circular polarization components is not only different from the linear components in nature but also altogether different for the different helicities of incident polarized light. These polarization dependences are basically the property of the forked grating. It does not depend on the birefringence of the film as we get similar behavior in vortex generation with a spatial light modulator (SLM, HOLOEYE, LC-R 2500), the materials having different birefringences. Due to these polarization dependences, the setup can work as a polarization discriminator or polarization filter.

Our experimental results show that a spatial mode selector, like a forked grating, ends up also acting as a polarization discriminator, which is a consequence of the inseparability between polarization and spatial modulation. This can be seen as one classical analogue of quantum entanglement [32,33]. Since the diffracted beam fields in our experiment are generic elements of the tensor product space $\mathrm{C}^2 \otimes \mathrm{L}^2(\mathrm{R}^2)$, polarization and spatial modulation are expected to be inseparable, which is evident in the nature of polarization curves for various diffracted modes. Our results illustrate very well the theory given in [32,33] for a Mueller matrix to be a physical Mueller matrix.

4. Conclusion

We observe the crossing of two polarization components for the incident polarization, indicating equal probability for two polarization components that may lead to a new technique for obtaining polarization-entangled photons. In addition, the same polarization behavior for the central order and vortices signifies that the spin angular momentum and orbital angular momentum of photons are not coupled. Polarization discrimination observed for various cases shows that the setup can work as a polarization filter. It is evident that CGH behaves as a weak diattenuator but has

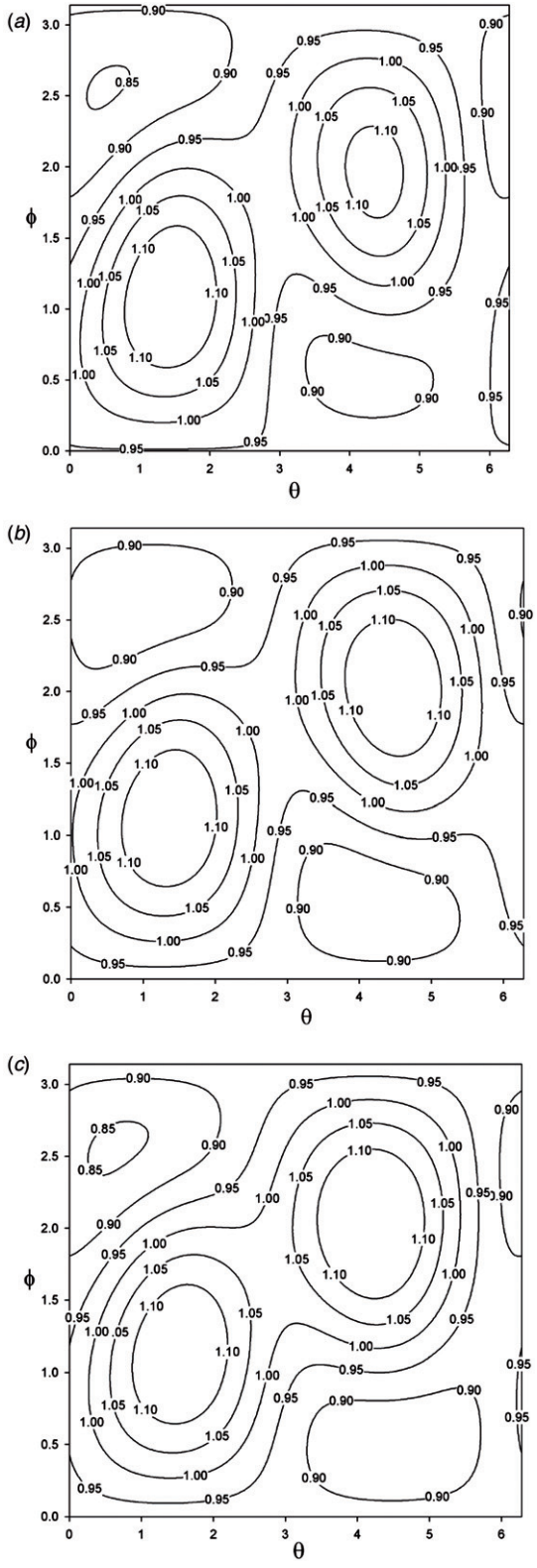

Figure 5. Contour plots for degree of polarization, $p(\theta, \varphi)$ for output light (*a*) vortex of order −1; (*b*) central order; and (*c*) vortex of order +1. θ runs from 0 to 2π while φ runs from 0 to π.

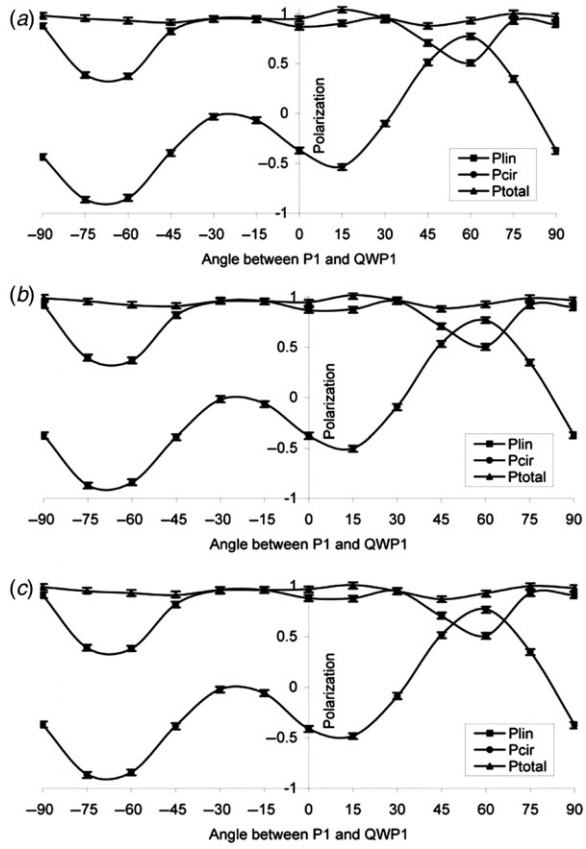

Figure 6. Variation of linear, circular and total polarization in each order (*a*) vortex of order −1; (*b*) central order; and (*c*) vortex of order +1 with incident polarization.

significant retardance for each diffracted order. CGH was also noticed as a helicity modification device.

References

[1] Soskin, M.S.; Vasnetsov, M.V. In *Progress in Optics*; Wolf, E., Ed.; Amsterdam: North-Holland, 2001; Vol. 42, pp 219–276.

[2] Arlt, J.; Dholakia, K.; Allen, L.; Padgett, J. *J. Mod. Opt.* **1998,** *45,* 1231–1237.

[3] Beijersbergen, M.W.; Coerwinkel, R.P.C.; Kristensen, M.; Woerdman, J.P. *Opt. Commun.* **1994,** *112,* 321–327.

[4] Beijersbergen, M.W.; Allen, L.; van der Veen, H.E.L.O.; Woerdman, J.P. *Opt. Commun.* **1993,** *96,* 123–132.

[5] Allen, L.; Padgett, M.J.; Babiker, M. In *Progress in Optics*; Wolf, E., Ed.; Amsterdam: North-Holland, 1999; Vol. 39, pp 291–372.

[6] Kuga, T.; Torii, Y.; Shiokawa, N.; Hirano, T.; Shimizu, Y.; Sasada, H. *Phys. Rev. Lett.* **1997,** *78,* 4713–4716.

[7] He, H.; Heckenberg, N.R.; Rubinsztein-Dunlop, H. *J. Mod. Opt*. **1995,** *42,* 217–223.
[8] Gahagan, K.T.; Swartzlander, G.A. *Opt. Lett*. **1996,** *21,* 827–829.
[9] Simpson, N.B.; Dholakia, K.; Allen, L.; Padgett, M.J. *Opt. Lett*. **1997,** *22,* 52–54.
[10] Galajda, P.; Ormos, P. *Appl. Phys. Lett*. **2001,** *78,* 249–251.
[11] Kivshar, Y.S.; Christou, J.; Tikhonenko, V.; Luther-Davies, B.; Pismen, L.M. *Opt. Commun*. **1998,** *152,* 198–206.
[12] Mair, A.; Vaziri, A.; Weighs, G.; Zeilinger, A. *Nature* **2001,** *412,* 313–316.
[13] Roychowdhury, S.; Jaiswal, V.K.; Singh, R.P. *Opt. Commun*. **2004,** *236,* 419–424.
[14] Nye, J.F.; Berry, M.V. *Proc. R. Soc. London A*. **1974,** *336,* 165–190.
[15] Freund, I. *Opt. Lett*. **2005,** *30,* 433–435.
[16] Singh, R.P.; Roychowdhury, S. *J. Mod. Opt*. **2004,** *51,* 177–181.
[17] Born, M.; Wolf, E. *Principles of Optics*; Cambridge University Press: New York, 1980.
[18] Kwiat, P.G.; Mattle, K.; Weinfurter, H.; Zeilinger, A.; Sergienko, A.V.; Shih, Y.H. *Phys. Rev. Lett*. **1995,** *75,* 4337–4341.
[19] Kwait, P.G.; Waks, E.; White, A.G.; Appelbaum, I.; Eberhard, P.H. *Phys. Rev. A* **1999,** *60,* R773–R776.
[20] Simon, R.; Sudarshan, E.C.G.; Mukunda, N. *Appl. Opt*. **1987,** *26,* 1589–1593.
[21] Erikson, W.L.; Singh, S. *Phys. Rev. E* **1994,** *49,* 5778–5786.
[22] Fainman, Y.; Shamir, J. *Appl. Opt*. **1984,** *23,* 3188–3195.
[23] O'Neil, A.T.; MacVicar, I.; Allen, L.; Padgett, M.J. *Phys. Rev. Lett*. **2002,** *88,* 053601.
[24] Lu, S-Y.; Chipman, R.A. *J. Opt. Soc. Am. A* **1996,** *13,* 1106–1113.
[25] Manhas, S.; Swami, M.K.; Buddhiwant, P.; Ghosh, N.; Gupta, P.K.; Singh, K. *Opt. Exp*. **2006,** *14,* 190–202.
[26] Sanjay Kumar, M.; Simon, R. *Opt. Commun*. **1992,** *88,* 464–470.
[27] Simon, R. *Opt. Commun*. **1982,** *42,* 293–297.
[28] Simon, R. *Opt. Commun*. **1990,** *77,* 349–354.
[29] Simon, R. *J. Mod. Opt*. **1987,** *34,* 569–575.
[30] Goldstein, D.H.; Chipman, R.A. *J. Opt. Soc. Am. A* **1990,** *7,* 693–700.
[31] Savenkov, S.N.; Klimov, A.S.; Oberemok, E.A. *J. Appl. Spectrosc*. **2009,** *76,* 743–751.
[32] Simon, B.N.; Simon, S.; Mukunda, N.; Gori, F.; Santarsiero, M.; Borghi, R.; Simon, R. *J. Opt. Soc. Am. A* **2010,** *27,* 188–199.
[33] Simon, B.N.; Simon, S.; Gori, F.; Santarsiero, M.; Borghi, R.; Mukunda, N.; Simon, R. *Phys. Rev. Lett*. **2010,** *104,* 023901.